Predation risk influences food-web structure by constraining species diet choice

Supporting Information

Hsi-Cheng Ho, Jason M. Tylianakis, Jonathan X. Zheng, and Samraat Pawar

April 17, 2019

Contents

1 Further details of the foraging models **2**
1.1 The classical optimal foraging model 2
1.2 The OF model 3
1.3 The PR Model 5
1.4 Foraging model parameterisation and structural schemes 5
1.5 Consumption rate threshold and predation-risk index in the PR model 8

2 Pseudocode for the OF and PR assembly processes **12**

3 Controlling the connectance of OF and PR webs via handling time magnitude **13**

4 Measurement of structural features **15**

5 Empirical food-web data **17**

6 Further details on data analyses **19**

7 Additional results **20**

8 Node-link diagram **26**

9 Trends in research on OFT-based food-webs **27**

1 Further details of the foraging models

Here we explain how we use classical optimal foraging theory (OFT) on species diet choice in this paper to obtain the OF and PR models, and how we parameterise these models.

1.1 The classical optimal foraging model

For simplicity, we first consider the case where a focal consumer preys on a single resource species, with per-capita units. Given the total searching time (T_s, the total time spent searching for resource items within a certain period of time, say, a foraging bout) and encounter rate (λ) between the consumer and the resource, we can derive the total number of resource items that a consumer can encounter per bout (R_{tot}) as:

$$R_{\text{tot}} = \lambda T_{\text{s}} \tag{S1}$$

with

$$\lambda = a'R, \tag{S2}$$

where a' is per-capita search rate and R the numerical density of the resource. In the original OFT work (Charnov & Orians 1973), it is assumed that once a resource item is encountered, it is captured instantly and successfully by the consumer, i.e., attack success probability (i.e., A in our OF & PR model in the main text) equals one. The total time spent foraging (T_{tot}, the length of a bout) is then

$$T_{\text{tot}} = T_{\text{s}} + T_{\text{s}}\lambda h' \tag{S3}$$

where h' is the per-capita handling time: the time taken by the consumer for pursuing, subjugating and ingesting one resource item. T_{tot} is nothing but the sum of searching time and handling time dealing with all captured resource items within a bout. Then, the per-capita intake rate during a foraging bout is the total number of resource items eaten (eqn (S1)) divided by the total foraging time (eqn (S3)):

$$\frac{R_{\text{tot}}}{T_{\text{tot}}} = \frac{T_{\text{s}}\lambda}{T_{\text{s}} + T_{\text{s}}\lambda h'} \tag{S4}$$

By cancelling T_{s} out from both the numerator and denominator, and replacing λ with eqn (S2), we get

$$\frac{R_{\text{tot}}}{T_{\text{tot}}} = \frac{a'R}{1 + a'Rh'} \ . \tag{S5}$$

This is the classical type-II functional response (Holling 1959) in per-capita units. Using this functional response equation, OFT stochastically models a series of decisions of the consumer, who either pursues or ignores each encountered resource item (of different types) such that its final diet composition maximises its net energy intake rate when averaged across many (sufficient from a sampling perspective) bouts. To illustrate this diet choice mechanism, let's introduce another resource species into the system. We now have two resources species, 1 and 2, identified by subscripts in the following equations. The profitability of the i^{th} resource species is how fast the consumer can gain energy from that item once it has been encountered. Let E_i be its energy content. Then, its profitability (p_i) is:

$$p_i = \frac{E_i}{h'_i} \tag{S6}$$

Note again that this is assuming attack success probability $A = 1$.

Now, let resource 1 be the more profitable resource among the two, such that:

$$p_1 > p_2, \text{ i.e., } = \frac{E_1}{h'_1} > \frac{E_2}{h'_2} \tag{S7}$$

We can calculate the consumer's energy intake rate (henceforth, consumption rate, C') by multiplying eqn (S5) by E, under three possible diet choice scenarios: eating only the more-profitable resource 1, eating only the less-profitable resource 2, or eating both:

$$\begin{aligned} C'_1 &= \frac{a'_1 R_1 E_1}{1 + a'_1 R_1 h'_1} \\ C'_2 &= \frac{a'_2 R_2 E_2}{1 + a'_2 R_2 h'_2} \\ C'_{12} &= \frac{a'_1 R_1 E_1 + a'_2 R_2 E_2}{1 + a'_1 R_1 h'_1 + a'_2 R_2 h'_2} \end{aligned} \tag{S8}$$

Given that resource 1 is more profitable (eqn (S7)), C'_2 is necessarily smaller than C'_{12}. Therefore, the consumer cannot achieve optimal (maximum) intake rate by eating only the less-profitable resource 2, and must always include the more-profitable resource 1 in its diet. The choice that the consumer needs to make then is whether or not to also include resource 2 into its diet. The criterion for resource 2 to be included is $C'_{12} > C'_1$, which can be re-written as:

$$a'_1 R_1 < \frac{E_2}{E_1 h'_2 - E_2 h'_1} \tag{S9}$$

because a', E, and h' are species-specific fixed values, the inclusion of resource 2 (the less-profitable resource) into the consumer's diet depends only on R_1, i.e., the density (or say abundance) of resource 1. Note the fact that the abundance of resource 2 itself is not relevant to its inclusion or not—only when resource 1 is rare enough should the consumer start to prey on resource 2.

From the above, we can summarise three diet-choice rules from classical OFT: (i) The most profitable resource species is always included in the consumer's diet regardless of its abundance. (ii) It is not because of the abundance of the less-profitable resource, but the rarity of the more-profitable resource, that the consumer includes the former into its diet. (iii) There is no way that the consumer "skips" species along the profitability ranking, that is, not eating the more-profitable resource but eating the less-profitable ones. All these rules also apply to our multi-species OF food web model below.

1.2 The OF model

The OF model is an extension of the above classical model to food webs. In this study, we decide to use biomass as the currency of energy for easier merging with metabolic theory. All parameters are therefore converted to mass-specific (i.e., per-biomass consumer on per-biomass resource) units as described below. The critical assumptions we make are that the energy content per unit biomass of resource, and conversion efficiency (i.e., from biomass to energy) of consumer, are both approximately constant irrespective of consumer or resource identity (Kondoh 2007; Petchey *et al.* 2008), and independent of body size (Peters 1986; DeLong *et al.* 2010; Lang *et al.* 2017).

Following eqn (S6) & (S7), for j^{th} consumer species, the profitability of an i^{th} resource species item (p_{ij}) is:

$$p_{ij} = \frac{A_{ij} E_i}{h'_{ij}} \tag{S10}$$

where E_i is the energy content of that resource item, and h'_{ij} here is the per-capita handling time as above (eqn (S3)). We explicitly include the A_{ij}, the attack success probability to capture that resource item, rather than implicitly assuming it equals one as in classical OFT (see above). That is, we relax classical OFT's assumption that encounter equals capture because the consumer's evaluation of profitability of a resource should in fact include its probability of successful capture. As we have assumed the energy content per unit biomass is constant for all species, E_i can be expressed as the resource item's body mass, m_i, multiplied by a constant that can be ignored as it has no effect on the relative profitabilities of species. Therefore, eqn (S10) can be re-written as:

$$p_{ij} = \frac{A_{ij} m_i}{h'_{ij}} \tag{S11}$$

We then divide both the numerator and denominator of eqn (S11) by m_i to convert it to profitability per unit resource biomass, and further convert it to consumer mass-specific profitability by multiplying the denominator by its body mass, m_j, to get:

$$p_{ij} = \frac{A_{ij}}{h_{ij}} \ . \tag{S12}$$

Here, h_{ij} is thus now resource mass-specific handling time (cf. h'_{ij} in above equations). Note that the above conversion does not change the relative profitabilities of resource species with respect to a focal consumer (i.e., resource profitabilites rank using eqn (S11) or (S12) is identical), but allows us to use the same mass-specific h_{ij} as when calculating consumption rate (see below and section 1.4). This value is also assumed to be independent from the effect of predation risk or any other factor.

In our study, we use biomass consumption rate as a proxy for energy intake rate, again, under the assumption that the energy content per unit biomass of resource is a global constant. The total biomass consumption rate of the j^{th} consumer species can therefore be written as:

$$\sum_{i \in D_j} \left(\frac{\epsilon a_{ij} A_{ij} X_i}{1 + \sum_{k \in D_j} a_{kj} A_{kj} h_{kj} X_k} \right) \tag{S13}$$

where D_j is the set of species in its diet, ϵ its conversion efficiency (here assumed constant), and, for its i^{th} resource species, a_{ij} is mass-specific search rate ($\text{m}^2 \cdot \text{kg}^{-1} \cdot \text{s}^{-1}$), A_{ij} its attack success probability, h_{ij} its mass-specific handling time (s), and X_i the resource's biomass abundance (density) ($\text{kg} \cdot \text{m}^{-2}$). Eqn (S13) is a multi-resource extension of the classical (single-resource) type-II functional response (as C'_{12} in eqn (S8) could be expressed in this form), and is the expected energy intake over a large sample of iterated, stochastically-spaced foraging bouts (Charnov & Orians 1973). Here again we include an explicit attack success probability, A, in comparison to the classical optimal foraging model with implicit $A = 1$. We also note that $A = 1$ is included as scheme 10 in our synthetic food-web analysis (see main text and section 7 below), so this study covers the classic optimal foraging model structure as well.

Just like the classical model (eqn (S8)–(S9)), the OF model determines the optimal diet by searching through all possible diet breadths along the profitability ranking (i.e., rule (iii) at the end of the previous subsection) and identifying the D_j that maximises eqn (S13), which presents the optimal diet.

1.3 The PR Model

As explained in the main text (eqn (2) & C_{risk}), the PR model extends the OF model by imposing predation risk and metabolic constraint (minimum consumption rate) on consumers' diet choice decisions. Given a risk of predation (eqn (S26)) and a minimum consumption rate (eqn (S25)), consumers can either narrow or broaden their diet. Narrowing the diet entails taking fewer resource species than the optimal set, i.e., fewer more energy-rich items that require less handling time overall. Broadening the diet entails taking more resource species than the optimal set, i.e., more energy-poor items that require more handling time overall. Under the assumption that handling is less risky than searching or waiting for prey, diet broadening in the PR model in effect results in a re-allocation of time within a foraging bout from searching/waiting to handling. That is, accepting less-profitable resources makes encounters with acceptable resource items more frequent, but the set of accepted items needs a longer time to handle overall. To make this explicit, consider the two-species OFT scenario above. From eqns (S3) and (S8), the total time spent foraging on resource 1 ($T_{\text{tot, 1}}$) versus on both resource 1 and 2 ($T_{\text{tot, 12}}$) are, respectively,

$$\begin{aligned} T_{\text{tot, 1}} &= T_{\text{s}} + T_{\text{s}} a_1' R_1 h_1' \\ T_{\text{tot, 12}} &= T_{\text{s}} + T_{\text{s}}(a_1' R_1 h_1' + a_2' R_2 h_2'). \end{aligned} \tag{S14}$$

In eqn (S14), given a fixed bout length (i.e., $T_{\text{tot, 1}} = T_{\text{tot, 12}}$), the T_{s} in $T_{\text{tot, 12}}$ must be smaller than the T_{s} in $T_{\text{tot, 1}}$ (i.e., less total searching/waiting time within a bout due to accepting resource 2), and meanwhile necessarily $T_{\text{s}}(a_1' R_1 h_1' + a_2' R_2 h_2')$ in $T_{\text{tot, 12}}$ is larger than $T_{\text{s}} a_1' R_1 h_1'$ in $T_{\text{tot, 1}}$ (i.e., more total handling time within a bout due to accepting resource 2).

The diet narrowing strategy involves the same logic applied in the opposite direction under the assumption that handling is riskier than searching/waiting. By such time-reallocation, the consumer reduces time spent performing riskier actions. Note that it is biologically possible that the consumer could change the bout length (T_{tot}) as a response to predation risk, which we have addressed in the "Discussion" section of the main text. Basically, it would not affect the diet breadth changing mechanism described here.

1.4 Foraging model parameterisation and structural schemes

Here we describe how the the foraging parameters of the OF and PR models—species biomass abundance (X_i), search rate (a_{ij}), attack success probability (A_{ij}), handling time (h_{ij}), and minimum consumption rate C_{min}—were specified. All quantities were eventually converted into mass-specific SI units (for values, see Table S1).

To quantify the model's sensitivity to variation in food-web attributes (species richness, proportion of basal species, mean and variation of species body masses) and specification of the foraging parameters, we developed schemes where these aspects were manipulated. Scheme 1 serves as a baseline. We describe its specification here, whereas each of the other schemes change one attribute or parameter with respect to scheme 1. These other schemes are are detailed in Table S2.

Biomass abundance (density)

Maximum species abundances generally follow Damuth's law (Damuth 1981; Peters 1986), with larger species having lower numeric densities:

$$X_i' = X_0 m_i^{-0.75} \tag{S15}$$

Here X_i' is the average population density (in individual/area or individual/volume) of species i. X_0 is a normalization constant. m_i is the average body mass of the i^{th} species . By multiplying eqn (S15) by m_i we can convert it into the scaling equation for species biomass density (in mass/area or mass/volume),

$$X_i = X_0 m_i^{0.25} \tag{S16}$$

We note that the X_0 (10^{-4} we used) and exponent (0.25) shown in eqn (S16) fall within the range of empirically-calculated values (Table S4). Indeed, in the case where we generated OF and PR counterparts of empirical food webs (the "Comparing ability of the foraging models to capture empirical food-web structure" section of main text) we did have empirical species biomass densities in seven webs (Table S4). However, because not all empirical webs had such data, for consistency we assigned biomass densities in all using Damuth's law. Eqn (S16) was applied with re-sampling variations in constant and exponent values in the empirical food webs section, and without such variation in the synthetic food webs section, as described in the main text. Using empirical biomass density values for X_i did not qualitatively change any of the results (results not shown).

Search rate

For mass-specific consumer j search rate (units of area/time or volume/time) we use (Pawar *et al.* 2012; Tang *et al.* 2014; Rizzuto *et al.* 2018):

$$\begin{aligned} a_{ij} &= 2V_0 d_0 m_j^{p_\text{v}+p_\text{d}-1} m_i^{p_\text{d}} \text{ in } 2D \\ a_{ij} &= \pi V_0 d_0^2 m_j^{p_\text{v}+2p_\text{d}-1} m_i^{2p_\text{d}} \text{ in } 3D \end{aligned} \tag{S17}$$

where V_0 and p_v are the normalization constant and exponent for the scaling of velocity, d_0 and p_d the constant and exponent of the scaling of reaction distance (at which the consumer and resource can sense and react to each other), and D is foraging (interaction) dimensionality. As such (S17) is the "grazing" version of the more general model of Pawar *et al.* (2012). We use this particular model for a throughout this study because it has been shown that the effect of foraging strategy is relatively small compared with the effect of foraging dimensionality (Pawar *et al.* 2012), and also because the majority of trophic interactions in the empirical food-web data we used were grazing.

Attack success probability

We phenomenologically model the attack success probability of species j attacking i as:

$$A_{ij} = \frac{1}{1+0.25e^{-m_j^{0.33}}} \left(\frac{1}{1+\left(\log_{10}\left(R_\text{p}\frac{m_j}{m_i}\right)\right)^2} \right)^{0.2} \tag{S18}$$

where R_p is the preferred resource-consumer body-size (body mass) ratio, and e is Euler's number. In the right hand side of eqn (S18), the first component is bounded between 0.8 and 1 (with the lower bound set by the constant 0.25) describes an monotonic increase of success probability with m_j, with the curvature regulated by the constant 0.33. The second component (bounded between 0 and 1) imposes a dome-shaped change in success probability with resource-consumer body-size ratio with its breadth controlled by the exponent 0.2. The value of this component peaks when the size-ratio equals R_p. Because size-ratios tend to be log-normally distributed, the $\log_{10}$ transformation guarantees that the decline is symmetric on either side of this ratio. This model (eqn (S18)) captures two biologically-realistic features of attack success: (i) large consumers tend to have higher success probability than small consumers, and (ii) the consumer's attack is more likely to succeed when the prey's body-size is appropriate, and less likely when the prey is too large or too small (*sensu* Caparroy *et al.* 2000; Vucic-Pestic *et al.* 2010; Pawar 2015). In other words, the probability peaks at a preferred body-size ratio. In this study, using different forms for A (i.e., scheme 8–10 in Table S2) did not qualitatively change our results (Section 7).

Handling time

According to Pawar *et al.* (2012), the consumer's per-capita handling time for resource biomass (i.e., the conventional per-capita handling time h' divided by resource body mass) is

$$h''_{ij} \propto m_j^{-\beta}, \tag{S19}$$

where β the scaling exponent of basal metabolic rate (Savage *et al.* 2004, 2007; Pawar *et al.* 2012). To make it mass-specific (i.e., per-biomass consumer on per-biomass resource), we multiply eqn (S19) by m_j to get

$$h_{ij} \propto m_j^{1-\beta}. \tag{S20}$$

where h_{ij} is mass-specific handling time. Furthermore, handing time should also be subject to biomechanical constraints imposed by resource-consumer size ratio. Therefore, we express handling time as

$$h_{ij} = h_0 m_j^{1-\beta} H\left(\frac{m_i}{m_j}\right) \tag{S21}$$

where h_0 is a constant. H is a U-shaped function which captures the fact that consumer should more easily handle a captured resource within an appropriate (preferred) size range with a peak at a particular, optimal resource-consumer body-size ratio. Just like A (eqn (S18)), handling time should be the lowest at a preferred body-size ratio and increase with deviation from that ratio. We use the inverse of a Gaussian probability density function, standardising the lowest point to 1, to capture this behaviour. For the preferred ratio, the same R_p as in attack success rate is used.

Another handling time parameterisation that also takes into account the body-size ratio influence, but with different logic and assumptions, can be found in the study by Petchey *et al.* (2008) on ADBM. Their "ratio handling time function" is

$$h'_{ij} = \begin{cases} \frac{h_0}{L - \frac{m_i}{m_j}} & \text{if } \frac{m_i}{m_j} < L \\ \infty & \text{otherwise.} \end{cases} \tag{S22}$$

Here h'_{ij} is consumer per-capita handling time on resource individual. h_0 again is a constant. L is the

largest consumable resource-consumer body-size ratio, beyond which the resource is considered too large to be consumed (i.e., with infinite handling time). A lower limit of handling time is set because no matter how small the resource item is ($\frac{m_i}{m_j} \to 0$), the consumer still needs a certain amount of time to handle it ($\frac{h_0}{L}$). Multiplying eqn (S22) by $\frac{m_i}{m_j}$ to convert it into mass-specific sense (i.e., per-biomass consumer on per-biomass resource), we get

$$h_{ij} = \begin{cases} \frac{h_0 m_j^2}{L m_j m_i - m_i^2} & \text{if } \frac{m_i}{m_j} < L \\ \infty & \text{otherwise.} \end{cases} \tag{S23}$$

Both types of handling time parameterisations, i.e., eqn (S21) and (S23), were included in the simulation schemes of this study (Table S4).

1.5 Consumption rate threshold and predation-risk index in the PR model

To maintain itself and survive, the energy intake of an individual should at least balance the continuous energy loss due to maintenance metabolism. This corresponds to the basal (survival/maintenance) metabolic rate (BMR, in energy/time) of an individual (Belovsky 1981; Peters 1986; Brown *et al.* 2004; Rizzuto *et al.* 2018)

$$\text{BMR} = B_0 m^{\beta} \tag{S24}$$

where B_0 is a coefficient that depends on taxon and temperature. In this study, as we used biomass density as the currency of energy, a basic biomass consumption rate threshold (C'_{min}) for individual consumer's survival could be drawn in proportion to BMR ($C'_{\text{min}} \propto \text{BMR}$). Dividing eqn (S24) by m to make it mass-specific, C_{min} (in 1/time) for species i can then be expressed as

$$C_{\text{i, min}} = C_0 m_i^{\beta - 1} \tag{S25}$$

where C_0 is a normalization constant. Biologically, this term (eqn (S25)) is the mass-specific biomass loss rate due to maintenance metabolism.

The amount of predation risk that a focal species experiences is quantified as a predation-risk index (P_{risk}), which is positively determined by the ratio of the total biomass of its realised consumers ($\sum X_{\text{real}}$) and the total biomass of all consumer species ($\sum X_{\text{all}}$)

$$P_{\text{risk}} = \left(\frac{\sum X_{\text{real}}}{\sum X_{\text{all}}} \right)^{e_{\text{P}}} \tag{S26}$$

where P_{risk} is bounded between 0 and 1 and is directly used for drawing a reference consumption rate for the diet broadening/narrowing effect described in the main text; e_{P} is an exponent that determines how P_{risk} increases along with the increasing $\sum X_{\text{real}}$, as shown in Fig. S1. Compared to the $e_{\text{P}} = 1$ case, P_{risk} will be smaller for the same $\sum X_{\text{real}}$ if $e_{\text{P}} > 1$, where the diet broadening/narrowing effect of the focal consumer species is thereby less sensitive to the change in the number (and thus $\sum X_{\text{real}}$) of its consumers (Fig. S1). This index is based on the rationale that, from a resource's point of view, the predation risk it suffers should increase with the number of consumer species in the environment that are preying on it, as well as the abundances of those consumers. We also note that by our assumption of allowing intraguild predation and cannibalism, all species share the same $\sum X_{\text{all}}$ value and therefore this predation-risk index presents a standardised evaluation of risk which could be compared among species. Species with fewer realised consumer species are likely to have lower P_{risk} than those with

many.

In the empirical food web section of the main text, we simulated model-generated counterparts of empirical food webs with given parameter values and $e_{\mathrm{P}} = 1$. Regarding controlling the connectance (see the main text and section 3), sometimes, for a replicate, even the largest h_0, based on which all species barely fulfil the $C_{\min}$ requirement (i.e., even larger h_0 leads to unfeasible species), is already used, the generated PR web is still over-connected. This can be seen as species being too sensitive to predation risk such that their diet broadens too fast. We therefore increased e_{P} by 0.25 to slightly weaken the diet-broadening effect (S1) in such cases. This process was repeated until a PR web with acceptable connectance was successfully generated. The simulated connectance values, along with the e_{P} used to achieve them, is summarised in Table S4. In the synthetic food web section, we did not limit the connectance of generated food webs, but just made sure that the three webs (i.e., the OF, PR, and null ones) share the same connectance. The values of e_{P} were therefore kept as scheme-dependent values (Table S4).

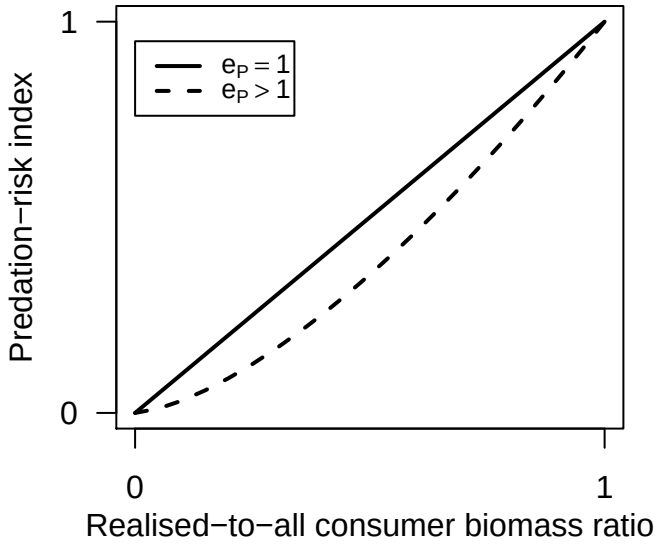


Figure S1: The effect of e_{P} on how predation-risk index (P_{risk}) is evaluated from the total realised-to-all consumer biomass ratio ($\sum X_{\mathrm{real}} / \sum X_{\mathrm{all}}$).

Table S1: Summary of parameters used in this work. Note that most of our foraging model parameters are derived from the underlying parameters listed in this table. These are further described in the text of this section.

Parameter	Definition	Value used	Unit	Reference
X_0	Biomass s.c.	10^{-4}	$kg^{0.75} \cdot m^{-2}$ for 2D; $kg^{0.75} \cdot m^{-3}$ for 3D	Pawar *et al.* 2012
V_0	Velocity s.c.	0.33	$m \cdot s^{-1} \cdot kg^{-p_v}$	Rizzuto *et al.* 2018
d_0	Reaction distance s.c.	1.62	$m \cdot kg^{-2p_d}$	Pawar *et al.* 2012; Rizzuto *et al.* 2018
p_v	Velocity s.e.	0.21		Pawar *et al.* 2012; Rizzuto *et al.* 2018
p_d	Reaction distance s.e.	0.21		Pawar *et al.* 2012; Rizzuto *et al.* 2018
R_p	Globally preferred body size ratio by consumers	0.1 for synthetic food webs; Median of empirical ratios for empirical food-web counterparts.		
β	Resting metabolic rate s.e.	0.75		Savage *et al.* 2007; Ritchie 2009; Pawar *et al.* 2012
h_0	Mass-specific handling time s.c.	Varied	$s \cdot kg^{-0.25}$	
L	The largest consumable body size ratio	1	$kg^{1-\beta} \cdot s^{-1}$	
C_0	Consumption rate threshold s.c.	4.15×10^{-8}	$kg^{0.25} \cdot s^{-1}$	Pawar *et al.* 2012
e_P	Predation-risk index exponent	Scheme dependent		

In the above table, s.c.: Scaling constant; s.e.: Scaling exponent.

Table S2: Schemes of generating synthetic food webs that we studied in this work. Each scheme stands for a specific combination of mathematical structure of food-web parameters (S, B, M_{mean}, M_{sd}, e_{B}) and foraging parameters (a, A, h, e_{P}). Scheme 1 presents a baseline settings for these parameters, whereas each of the following schemes vary one parameter from scheme 1 while keeping others the same.

Scheme	S	B	M_{mean}	M_{sd}	e_{B}	a	A	h	e_{P}
1	50	0.1	10^{-5}	10	0.25	2D of eqn. (S17)	Eqn. (S18)	Eqn. (S22)	1
2	150								
3		0.4							
4			10^{-10}						
5				10^{3}					
6					0				
7						3D of eqn. (S17)			
8							Only 2nd component of eqn. (S18)		
9							Only 2nd component of eqn. (S18)*		
10							1		
11								Eqn. (S21)**	
12								Eqn. (S23)	
13									0.5
14									2

In the above table, S: Species richness; B: Proportion of basal species; M_{mean} and M_{sd}: Mean and standard deviation of the log-normal distribution from which species body masses were drawn; e_{B}: Biomass scaling exponent; a: Search rate; A: Attack success probability; h: Handling time; e_{P}: Predation-risk index exponent (eqn (S26)).

*: The dome-shaped component of eqn (S18), but with the exponent changed from 0.2 to 1 so that the dome becomes steeper.

**: The standard deviation of the inverse Gaussian probability density function, H of eqn (S21), changed from 1 to 1.1 so that the U-shape becomes less steep.

2 Pseudocode for the OF and PR assembly processes

Here we present the pseudocode for our assembly algorithm. Note that this entire process is repeated for multiple values of handling time h in order to achieve a preset connectance. Stopping after line 3 results in an OF web, while continuing results in a PR web. An explanation for the various values of C on line 7 is in Fig. 1 of the main text.

input : Set of species $S = \{1 \dots n\}$, their biomasses $m_{\{i \in S\}}$, set of basal species $B \subset S$
output : PR food web diets $D_{\{i \notin B\}}$

1 **foreach** consumer species $i \notin B$ **:**
2 Order other species by profitability defined by eqn (S12)
3 Initialise diet D_i by adding species in descending order until eqn (1) is maximised
4 **until** all D_i do not change **:**
5 **foreach** consumer species $i \notin B$ **:**
6 Calculate $P_{i,\text{risk}}$ using eqn (2)
7 Risk-compromised consumption $C_{\text{risk}} = C_{\text{surv}} + (1 - P_{\text{risk}})(C_{\text{opt}} - C_{\text{surv}})$
8 Re-assign diet D_i by broadening to the closest $C(D_i) \geq C_{\text{risk}}$

3 Controlling the connectance of OF and PR webs via handling time magnitude

In this section, we explain how the connectance of model-generated web, for both the OF and PR model, was controlled by manipulating the magnitude of handling time.

The handling time for every resource-consumer pair is given by eqn (S21) explained in section 2. Given a h_0 value and other parameters, the consumption rate of any focal consumer across all its possible diet breadth can be calculated by using eqn (1) of the main text, as we did in main text Fig. 1 and Fig. S2 here. As the magnitude of handling time is increased by giving a larger h_0 value, the consumer's consumption rate for every possible diet breadth decreases due to the larger denominator of eqn (1). At the same time, the maximum consumption rate shifts to be at a narrower diet set, which means that the optimal diet breadth becomes narrower. This is purely a mathematical outcome of the multi-resource type-II functional response, i.e., eqn (1). Under the OFT diet-choice rule where consumer take the optimal diet set, assigning a large-enough h_0 guarantees that the focal consumer will definitely consume only the most profitable resource (Fig. S2 rightmost), whereas a small-enough h_0 make the consumer eat everything (Fig. S2 leftmost).

Extrapolating the above to all consumer species in the community, the food-web connectance will be higher if all consumers have broader diet, and vice versa. The connectance of the OF and PR model (as PR starts with an OF-derived initial web) can therefore both be manipulated by assigning the value of h_0. Given the same set of species and parameters, the two models reach the same connectance with different h_0 values, where the PR needs a larger one due to the diet-broadening strategy. We thus control the connectance of output food webs via assigning proper h_0 values as decribed in the main text, so that the structural comparison could be conducted with webs that share the same connectance.

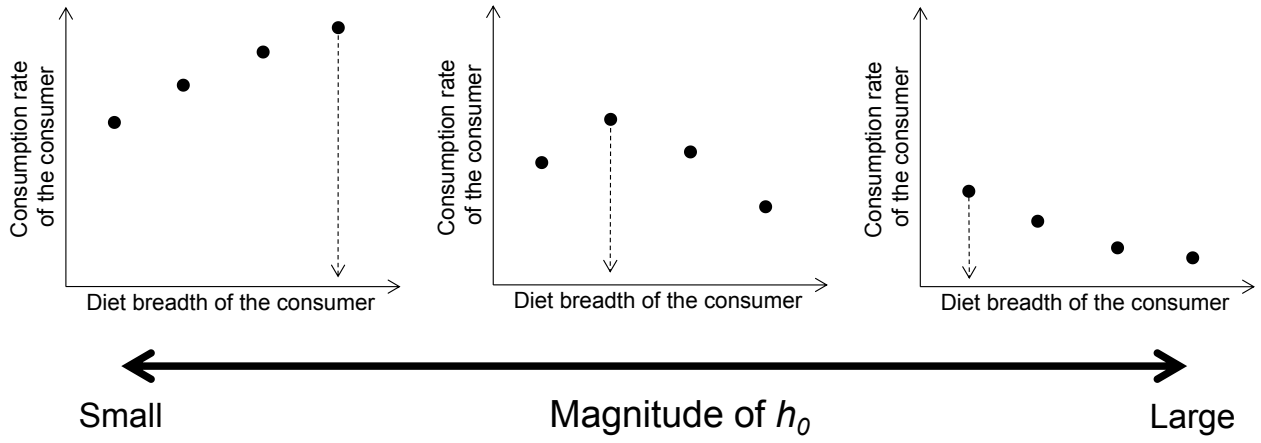


Figure S2: Illustration of how consumption rate of the consumer is influenced by the magnitude of h_0. With larger h_0, the handling time of every resource-consumer pairs increase evenly. For a focal consumer, this results in a decrease in consumption rate across all possible diet breadth (i.e., all points move downward), meanwhile the optimal diet becomes narrower (i.e., the peak shift leftward).

Note that we set the connectance of the PR web first then match the connectance of OF/null web with it. The reason is that, in the PR assembly, species' diet breadths and predation-risk index values iteratively change each other until they reach a steady state. Thus, the connectance of PR food webs responds less smoothly but step-wise to variation in h_0. It is therefore more difficult to generate a PR

web with exactly the desired connectance. The OF assembly, on the other hand, can easily achieve a desired connectance by assinging a proper h_0 value. The null webs are randomly connected and we can directly assign their connectance. Therefore, matching the connectance of the latter two to the PR value is a practical way to have them share the same connectance.

4 Measurement of structural features

We summarise the food-web metrics used in this study in Table S3.

We note that in this study we focus on nestedness and modularity because these are arguably the most well-reported empirical food-web properties, as stated in main text, and also because such structural features quantify the pattern of how trophic links are distributed among species, which directly reflects species' diet choice.

Table S3: Food-web structural metrics used in this study.

Metric	Definition	Quantifying measurement	Reference
Nestedness	Express the food web as a consumer-resource bipartite network, nestedness is the degree that some species' diet being subsets of other's diet.	NODF: use `nestednodf` function of the R package `vegan` (ver. 2.5-2).	Johnson *et al.* 2013; Oksanen *et al.* 2018 (`vegan`); Ulrich & Gotelli 2007
Modularity (compartmentalisation)	The degree of having compartments, which are subgroups of species where many linkages take place within but a few between.	Modularity index: use `cluster_walktrap` function with `modularity` function of the R package `igraph` (ver. 1.2.1).	Csardi & Nepusz 2006 (`igraph`); Krause *et al.* 2003
Clustering (transitivity)	The degree to which species form close-knitted groups with high density of linkages.	Clustering coefficient: use `transitivity` function of the R package `igraph` (ver. 1.2.1).	Csardi & Nepusz 2006 (`igraph`); Opsahl & Panzarasa 2009
Coherence	The degree of homogeneity of the difference between the trophic levels of every resource-consumer pair within the web.	Incoherence index: the SD of the distribution of trophic distance of all linkages. The trophic distance is the difference in trophic level between the conusmer and the resource of a linkage. Note that this index has a lower bound of 0 and is inversely reflecting the level of coherence.	Johnson *et al.* 2014
Trophic similarity	The extent that species overlap in the trophic role the play in the food web.	The web-averaged species-pair similarity, which is the number of shared consumers and resources of the focal pair divided by their total number of consumers and resources in combination.	Williams & Martinez 2000
Trophic level	The distance of a species it is from the bottom of the food web.	Prey-averaged levels: the level of a species is the average level of all its resources plus 1. The level of basal species are assigned as 1.	Williams & Martinez 2004
In degree (generality)	Resource count of a consumer; the number of linkages that connect to resources of a species.	As left.	
Connectance	The proportion of realised linkages out of all possible linkages of a web.	Number of linkages divided by the square of species richness.	Dunne *et al.* 2002a,b

5 Empirical food-web data

We compiled data on 12 empirical food webs from published works (Table S4). These webs were all resolved to the species level. For CSM, BSQ, and EPB, the original data partly includes life-stage level resolution on trophic interactions among species. We collapsed these 3 webs to species level to stay in accordance with the other webs, by summing up the biomass and diet of any species across all its life stages. We included only carnivorous, herbivorous, and detritivorous links. The number of species in these webs ranges from 28 to 251, and web connectance ranges from 0.018 to 0.294. Note that we present the biomass scaling relationship of the seven webs for which we have information on empirical biomass densities, but in our work we reassign the biomass densities of all using Damuth's law as described in section 1.4.

Table S4: Summary of the empirical food web datasets used in this study.

Name (abbr.)	No. nodes	No. consumers	No. linkages	Environment	Empirical C	Simulated C	Median RC	e_P	Empirical c_B	Empirical e_B	Reference
Bahia San Quintin (BSQ)	170	115	1290	Mixed	0.055	0.056 ± 4.4E-4	5E-4	1.115 ± 0.086	1E-4.754	0.134	Hechinger *et al.* 2011
Broadstone Stream (BSS)	28	9	138	Freshwater	0.176	0.170 ± 0.002	0.081	1.075 ± 0.068	1E-3.525	0.236	Woodward *et al.* 2005
Caribbean (Car)	248	241	3241	Marine	0.053	0.053 ± 5.3E-5	0.012	1	1E-3.526	0.011	Bascompte *et al.* 2005
Carpinteria Salt Marsh (CSM)	154	111	1303	Mixed	0.068	0.068 ± 1.4E-5	1.4E-3	1	1E-4.482	0.214	Hechinger *et al.* 2011
Estero de Punta Banda (EPB)	203	145	2368	Mixed	0.075	0.075 ± 7.5E-5	4.9E-4	1	1E-4.753	0.090	Hechinger *et al.* 2011
Grand Caracaie (GC)	87	49	608	Marsh	0.08	0.081 ± 5.4E-4	0.263	1.065 ± 0.031	--	--	Brose *et al.* 2005
Gearagh Woodland (GW)	105	91	357	Terrestrial	0.032	0.033 ± 3.1E-4	0.31	2.105 ± 0.126	1E-2.200	0.812	McLaughlin *et al.* 2010
Kongsfjorden (Kon)	251	91	1144	Marine benthic	0.018	0.018 ± 1.2E-4	0.014	1.205 ± 0.068	--	--	Renaud *et al.* 2011
Skipwith Common (SC)	33	18	320	Freshwater	0.294	0.289 ± 4.7E-3	0.166	1.456 ± 0.238	--	--	Brose *et al.* 2005
St. Marks (StM)	96	69	783	Estuarine	0.085	0.088 ± 8.1E-4	0.006	1.285 ± 0.073	--	--	Christian & Luczkovich 1999
Tuesday Lake 1984 (TL84)	50	25	269	Freshwater	0.108	0.108 ± 0.001	6E-4	1.035 ± 0.061	1E-3.748	0.103	Jonsson *et al.* 2004
Ythan Estuary 1996 (YE96)	79	59	264	Estuarine	0.042	0.044 ± 5.2E-4	2.1E-4	1.355 ± 0.171	--	--	Huxham *et al.* 1996; Leaper & Huxham 2002

In the above table, C: connectance; RC: resource-consumer body-size ratio; e_P: predation-risk index exponent; c_B: biomass scaling constant; c_B: biomass scaling constant; e_B: biomass scaling exponent.
For simulated C and e_P, mean ± 95% CI of the 50 simulations are shown.

6 Further details on data analyses

The measurements in this study (including those of additional results, see the next section), except TL-Mass (trophic level to log consumer body mass relationship) and ID-Mass (in-degree to log consumer body mass relationship), were analysed using linear mixed model (LMM) and paired-Wilcoxon tests to check for the difference among models. For the empirical part we focused on the absolute deviations from the empirical value and took these as the observations to evaluate model predictive performance. For the overall comparison of model performances (i.e., results in Fig. 2 of the main text), we used LMM with the type of model (i.e., OF and PR) as the fixed effect, and community (i.e., the 12 empirical ones) and iteration (50 for each community) as nested random intercept effects. For the community-based comparison, deviations are paired by iterations and analysed using a Wilcoxon test.

For the synthetic part, on the other hand, we directly compare the measurements to show the structural difference among models. Just as the corresponding observations (i.e., among models but from the same iteration) in the empirical part were derived from the same set of re-drawn parameters, in the synthetic part they were derived from the same synthetic community, and thus were not independent to each other. We thus set the type of model (i.e., OF, PR, and null) as the fixed effect, but the identity of iteration as a random intercept effect in the synthetic part, and reported the significance of difference between the OF and PR models. Notably, the measurement here may be transformed to meet the normality assumption of LMM. We first checked residual (i.e., of LMM model) normality of original readings using a Shapiro-Wilk test, and if it was violated, we further applied 4 transformations and picked the one that gave the largest p-value of normality tests for analysis. Possible data types are: Original, Square-root transformed, Log transformed ($\log_{10}(value)$ or $\log_{10}(value+1)$ if there is zero in the values), Reverse transformed ($-1/value$ or $-1/(value+1)$ if there is zero in the values), and Arcsine-square-root transformed (if the original values are not bounded between 0 and 1, they are standardised by dividing by the maximum reading (or 100 in NODF case), then taking the $\sin^{-1}\sqrt{value}$). The final adopted data type of the LMM analysis is indicated in Fig. S5–S7.

For TL-Mass, LMM were applied to visualise the relationship, where we took species body mass (in log scale) and the type of model as fixed effects with interaction, with the identity of iteration as a random effect. The random effect was set to be either on the intercept, the slope, or both, depending on which structure yielded the smallest AIC. For ID-Mass, as the relationship was not linear, we used a generalized additive mixed model (GAMM) to visualise the relationship. The type of model was set as a linear fixed predictor, while species body mass (in log scale) of each model type was set as a smooth predictor, and the identity of iteration as a random smooth.

The LMM was done by using `lmer` function of R package `lme4` (ver. 1.1-17, Bates *et al.* 2015). The GAMM was done by using `gam` function of R package `mgcv` (ver. 1.8-24, Wood 2006). Paired-Wilcoxon and Shapiro-Wilk tests were conducted using R-inbuilt functions.

7 Additional results

Here we firstly present the same result of Fig. 2 of the main text, except with standardised absolute deviation (Fig. S3). The results are qualitatively the same. We note that we were not comparing the deviation between nestedness and modularity, but between the two foraging models. As long as the deviations are paired-calculated with empirical values, we can judge if it is statistically different from 0 and if any of the OF/PR have smaller deviations (as an indication of better predictive performance), so standardisation is not necessary. However, using standardised values provides hints of how large the deviations are, relative to the empirical value.

Besides the focal structural measures of nestedness and modularity, we also measured several other food-web structural metrics and performed the same comparisons as described in the empirical and synthetic food webs sections of the main text. We note that the metrics we measured cover much of the same structural information as in the previous works, such as the ADBM studies (Beckerman *et al.* 2006; Petchey *et al.* 2008). The results of these are as shown in Fig. S4–S7, and the relevant terminology definitions can be be found in Table S3.

The PR model predicts clustering closer to the empirical value, while for coherence and trophic similarity there is no obvious superiority of predicting performance (Fig. S4). The synthetic part shows that the PR food webs are consistently more clustered, more coherent, and have higher similarity among nodes than OF food webs (Fig. S5).

For the resource-consumer body-size ratio-related features, we compared the median and standard deviation of resource-consumer body-size ratio distribution among the models. These features provide insights into how different-sized species and linkages are distributed within the food web. For the comparison with empirical food webs, there is no obvious pattern for the median of the ratio. For the standard deviation of the ratio distribution, empirical food webs tend to adopt higher value than the models' prediction. The PR model outperforms OF in 9 out of 12 empirical communities (Fig. S4). For the comparison among synthetic food webs, because of the body-size constraints embedded in A and h, both foraging models produced more constrained ratio distributions than the null webs, that is, with much smaller standard deviation. The comparison between the two foraging models showed that the PR model tended to produce food webs with higher median resource-consumer body-size ratio and higher standard deviation of that ratio, i.e., a wider and flatter ratio distribution, than the OF model (Fig. S5).

With regard to node-level features, we checked the relationships of consumer species' trophic level and in-degree against their log body mass (TL-Mass and ID-Mass, respectively) to inspect how these two node-level features varied with body mass. In-degree is the number of resources of a node, which directly reflects the diet breadth of species, so was considered as an important node feature in the diet-predicting context of this study. In general, empirical food webs tend to adopt a positive TL-Mass relationship and a dome-like ID-Mass relationship—not perfectly humped, but qualitatively higher in the middle than in the ends (Fig. S4), and the model-predicted webs reflect such a characteristic (Fig. S4, S5).

As stated in the main text, biologically, a species can either broaden or narrow its diet breadth as a response to predation risk, and we mainly focused on the former. We also conducted the same simulation using the PR model which is set to have the diet-narrowing effect. In a food web, however, if the consumers' diet become narrower, the resources species' predation risk will decrease, which will lead to further diet narrowing of these resource species and lower the predation risk downstream. This is exactly the opposite of the positive feedback between diet breadth and predation risk that happens

in diet-broadening case (as described in the main text), so the effect of predation risk tends to mitigate itself here. As a result, the predicted food webs of diet-narrowing PR model converges to OF, and the structural outcomes of the two models are almost identical (Fig. S6). If allowing the PR model to select the diet that gives the closest consumption rate to the risk threshold C_{risk} (i.e., could either be broadening or narrowing), because the diet-narrowing effect again diminishes, the results of this either-direction PR model (Fig. S7) largely converges to the diet-broadening case (Fig. S5).

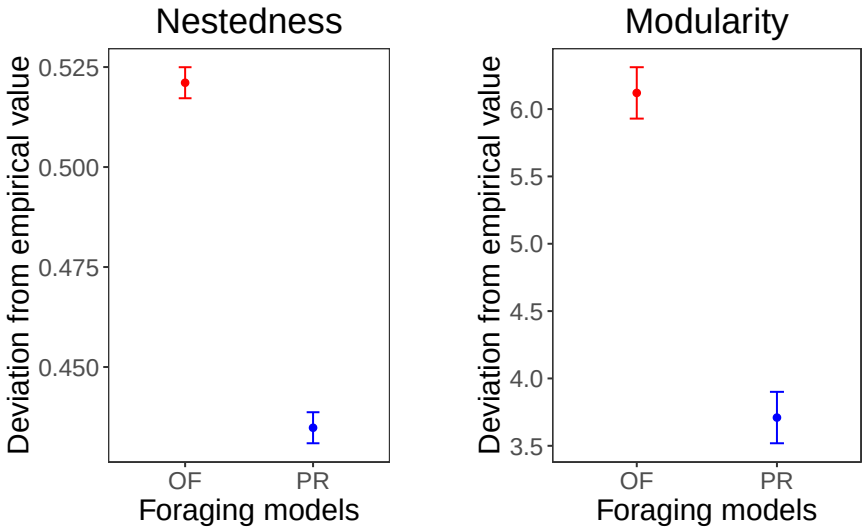


Figure S3: Performance of the Optimal Foraging (OF) and Predation Risk-Compromise (PR) models in predicting nestedness and modularity of empirical food webs. We evaluate the performance using standardised absolute deviations from the empirical value of both foraging models, which is the absolute value of the difference (of NODF and modularity index) between the model-generated web and the empirical web, divided by the reading of the empirical web. These are shown as mean ± 95% CI (LMM fixed-effect uncertainty only). The PR model has deviations significantly smaller than those of the OF model in both nestedness and modularity measurements ($p < 0.001$ in both cases), indicating a better predictive ability.

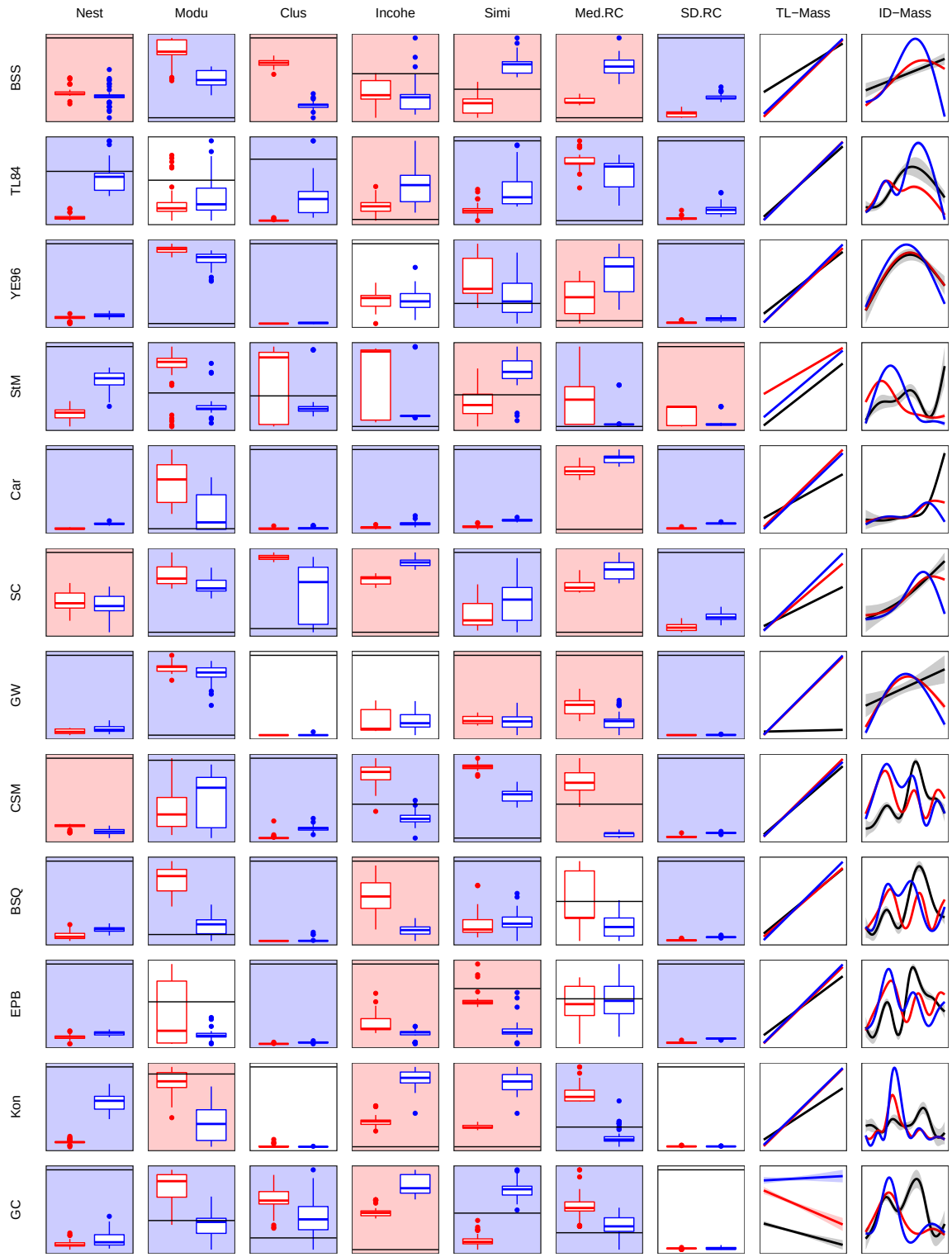


Figure S4: Summary of the structural features (as columns) of empirical food webs (as rows) and their OF and PR counterparts. Nest: level of nestedness (as NODF); Modu: level of modularity (as modularity index); Clus: clustering coefficient; Incohe: Incoherence index; Simi: web-averaged species-pair similarity; TL-Mass: Trophic level to log consumer body mass relationship; ID-Mass: In-degree to log consumer body mass relationship. Food-web name abbreviations are in accordance with Table S4. Red, blue, and black colour refer to OF, PR, and empirical food webs, respectively. The solid line present the mean or regression line, with corresponding shade present the 95% CI. The box plots present the model-generated values. Except in TL- and ID-Mass, the background of the plots are coloured in red/blue shade to point out which of OF and PR measurement mean values is significantly closer ($p < 0.05$) to the empirical value based on paired-Wilcoxon tests.

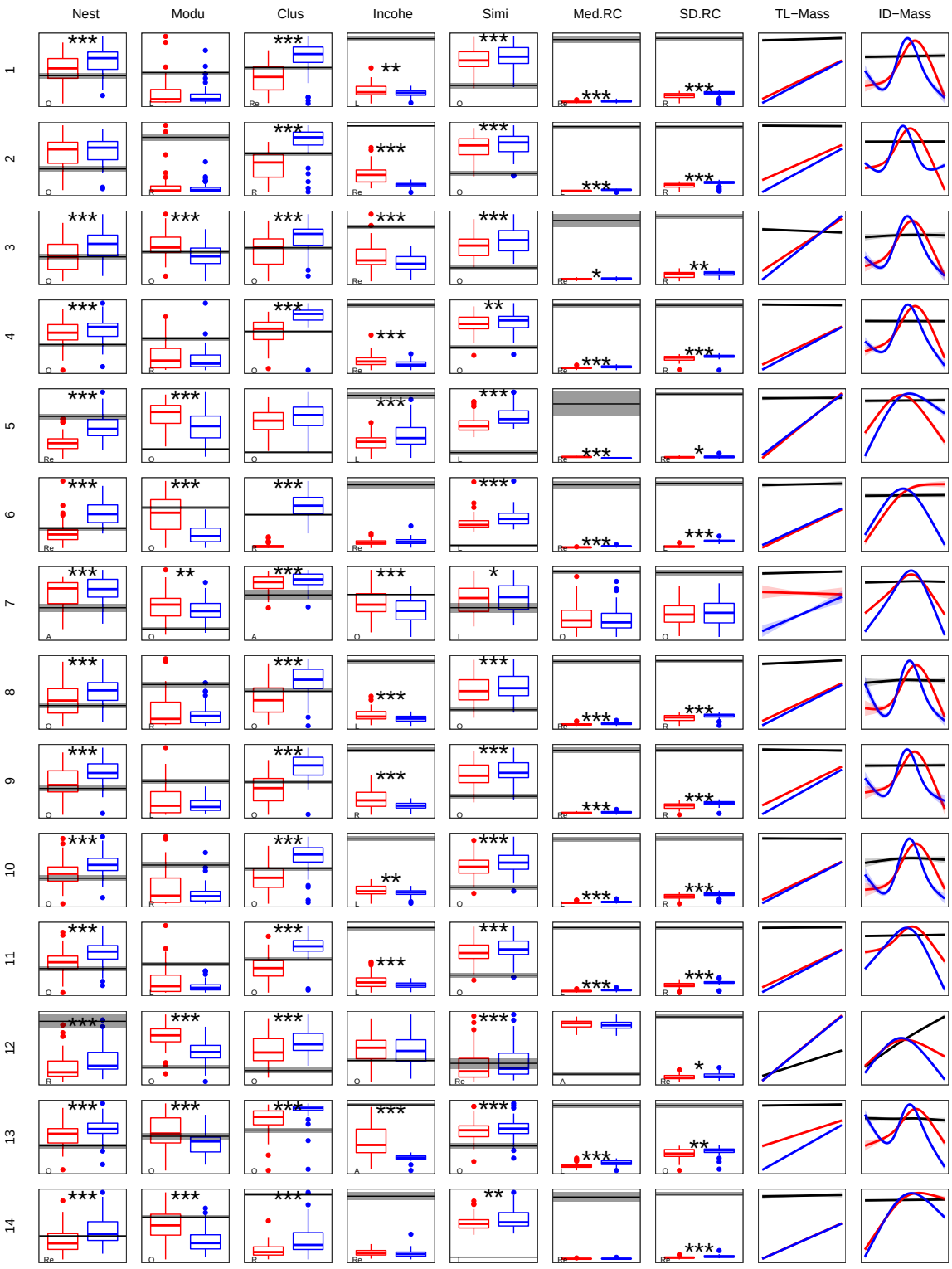


Figure S5: Summary of the structural features (as columns) of the OF, PR, & null food webs across all schemes (as rows). Measurement abbreviations are in line with Fig. S4. Red, blue, and black colour refer to OF, PR, and null food webs, respectively. The sold line with corresponding shade presents the mean ± 95% CI of observations or the regression line, whereas the box plots present the model-generated observations. The asterisks indicate whenever the OF/PR values are significantly larger than the other (*: $p < 0.05$; **: $p < 0.01$; ***: $p < 0.001$. LMM results). Adopted data type is indicated at the bottom left of the plots: O(original), R(square-root), L(log), Re(reverse), and A(arcsine square-root). Across schemes, there are consistent structural differences between OF and PR food webs despite of the variation in model mathematical structure and parameters.

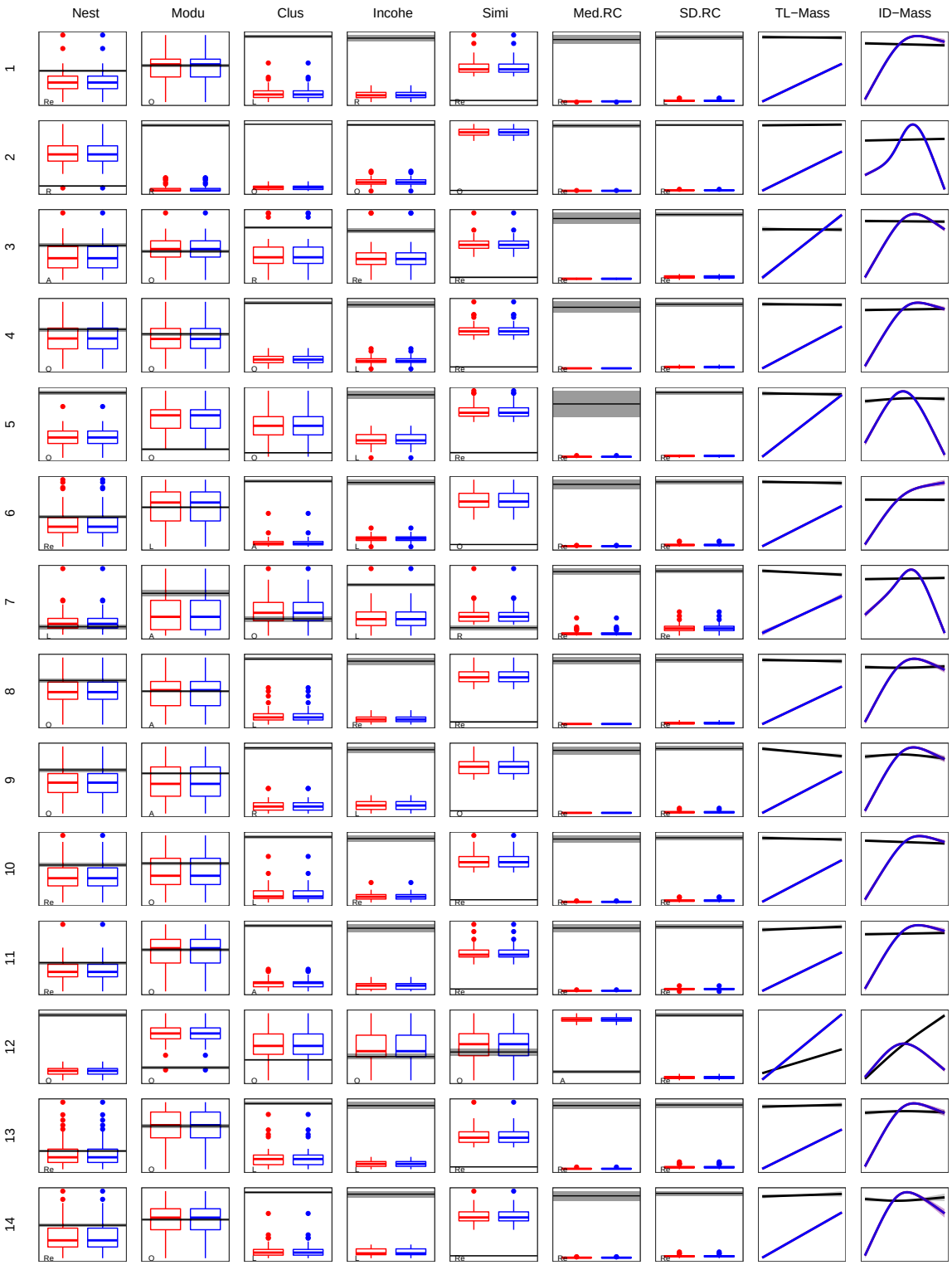


Figure S6: Summary of the structural features (as columns) of the OF, PR, and null food webs across all schemes (as rows), where in the PR model the predation risk is set to have diet-narrowing effect. All notations are in line with Fig. S5. As the PR in this case largely converge to the OF, the results show no difference between the two.

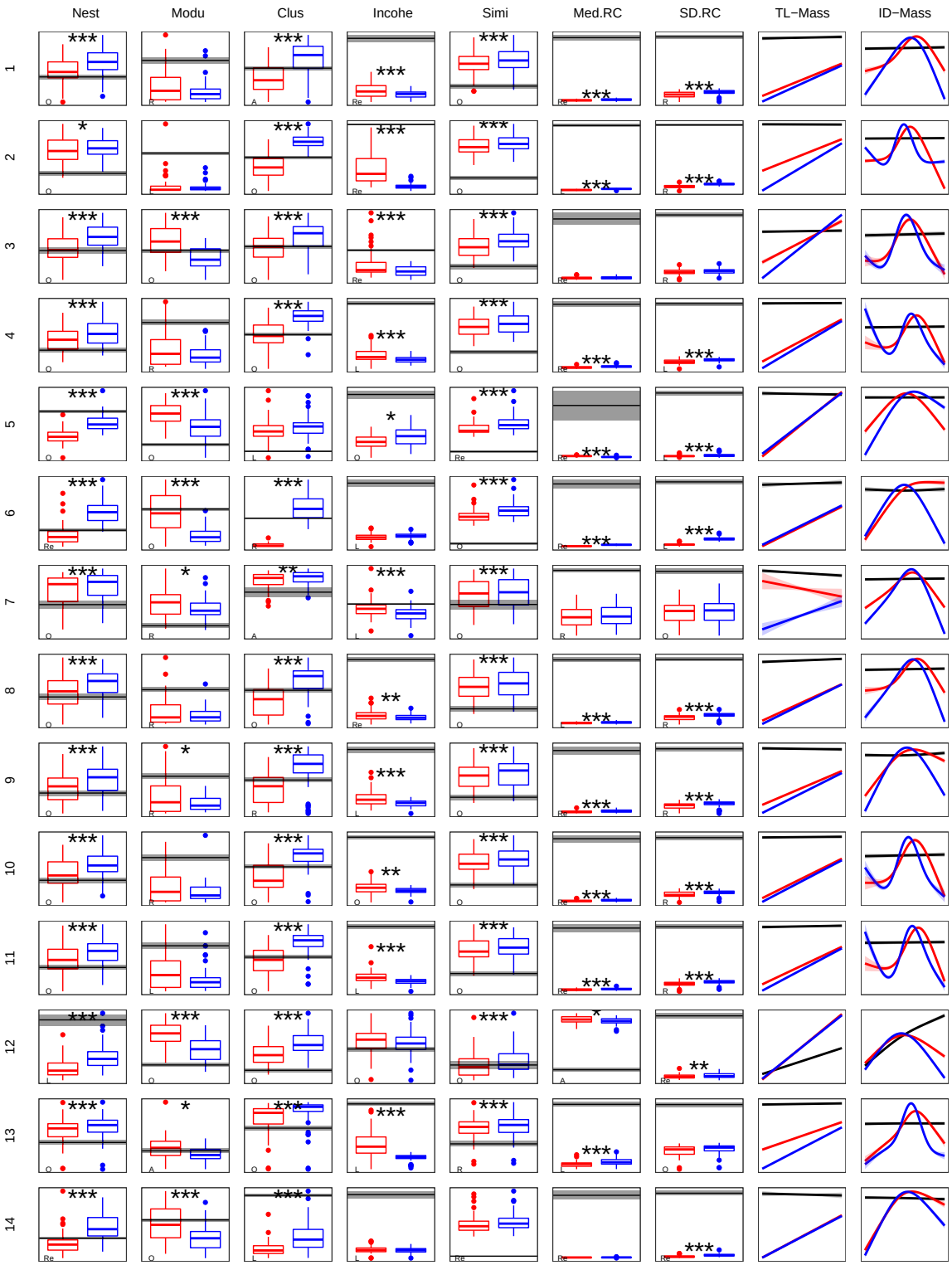


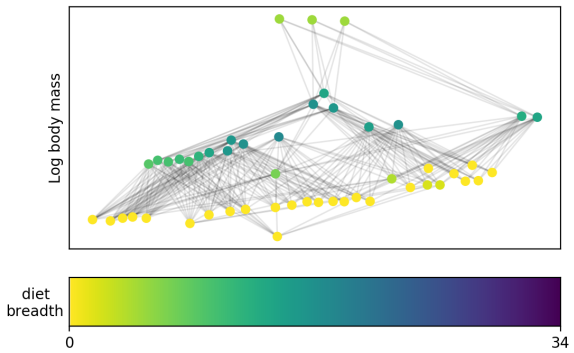
Figure S7: Summary of the structural features (as columns) of the OF, PR, & null food webs across all schemes (as rows), where in the PR model the predation risk is set to have either diet-narrowing or diet-broadening effect depending on which gives the closer consumption rate to the reference value. All notations are in line with Fig. S5. The results are largely the same with pure diet-broadening case as in Fig. S5.

8 Node-link diagram

The node-link diagram showed in Fig. 5 of the main text was produced by using the visualisation algorithm developed by Zheng *et al.* (2018). For ease of comparison, the x-position of nodes of all three diagrams are calculated based on connectivity information of the empirical food web such that the location of the nodes are fixed across diagrams.

Here with Fig. S8, we further show the diagrams of the same OF and PR food webs, but based on the PR web's connectivity information instead (i.e., the same webs as in Fig. 5B–C of the main text but plotted in another way with another set of x-position of nodes), which provided another visualisation of the difference between the OF and PR webs. Because we kept the connectance of the two webs the same, the OF and PR webs can be seen as the linkages being re-allocated among nodes from each other. Consequently, median-sized consumers have a broader diet in the PR than in the OF food web (e.g., the nodes that form a little triangle in the middle of Fig. S8), while the reverse is true for larger and smaller consumers (e.g, the three nodes at the top, and the two greenish nodes sitting right above the yellowish layer of nodes of Fig. S8, respectively)

(A) OF: optimal foraging model



(B) PR: optimal foraging model with predation-risk effect incorporated

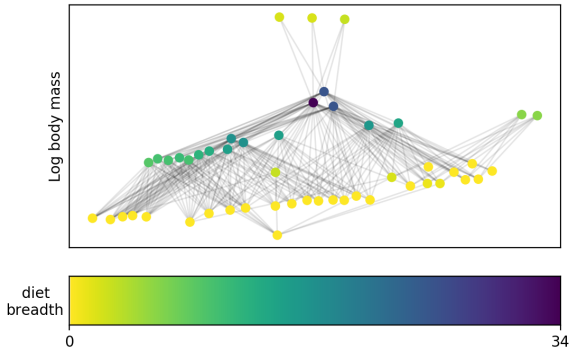


Figure S8: Node-link diagrams of the OF and PR food webs, corresponding to Fig. 5 of the main text.

9 Trends in research on OFT-based food-webs

Research on OFT-based food-webs has gradually faded from the literature after reaching a peak around 2010–2012. We searched literature using the Web of Science engine, with "optimal foraging" and "food web" as key words of the topics, then plot the number of found publications with the year they are published.

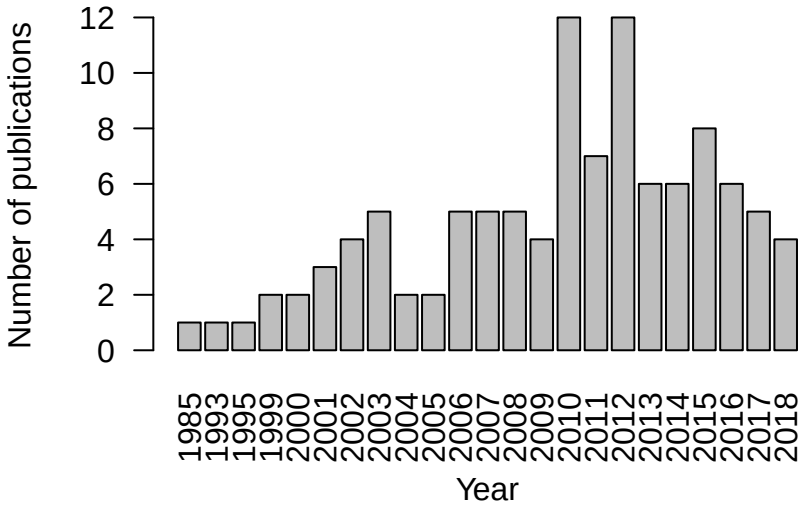


Figure S9: Number of research papers by year of publication with "optimal foraging" and "food web" as topic key words, searched by Web of Science.

References

Bascompte, J., Melián, C. J. & Sala, E. (2005). Interaction strength combinations and the overfishing. *Proceedings of the National Academy of Sciences of the United States of America*, 102, 5443–5447.

Bates, D., Mächler, M., Bolker, B. & Walker, S. (2015). Fitting linear mixed-effects models using lme4. *Journal of Statistical Software*, 67, 1–48.

Beckerman, A. P., Petchey, O. L. & Warren, P. H. (2006). Foraging biology predicts food web complexity. *Proceedings of the National Academy of Sciences*, 103, 13745–13749.

Belovsky, G. E. (1981). Food plant selection by a generalist herbivore: the moose. *Ecology*, 62, 1020–1030.

Brose, U., Cushing, L., Berlow, E. L., Jonsson, T., Banasek-Richter, C., Bersier, L.-F., Blanchard, J. L., Brey, T., Carpenter, S. R., Blandenier, M.-F. C., Cohen, J. E., Dawah, H. A., Dell, T., Edwards, F., Harper-Smith, S., Jacob, U., Knapp, R. A., Ledger, M. E., Memmott, J., Mintenbeck, K., Pinnegar, J. K., Rall, B. C., Rayner, T., Ruess, L., Ulrich, W., Warren, P., Williams, R. J., Woodward, G., Yodzis, P. & Martinez, N. D. (2005). Body sizes of consumers and their resources. *Ecology*, 86, 2545–2545.

Brown, J. H., Gilloolly, J. F., Allen, A. P., Savage, V. M. & West, G. B. (2004). Toward a metabolic theory of ecology. *Ecology*, 85, 1771–1789.

Caparroy, P., Thygesen, U. H. & Visser, A. W. (2000). Modelling the attack success of planktonic predators: patterns and mechanisms of prey size selectivity. *Journal of Plankton Research*, 22, 1871–1871.

Charnov, E. L. & Orians, G. H. (1973). *Optimal foraging: some theoretical explorations*. University of Washington.

Christian, R. R. & Luczkovich, J. J. (1999). Organizing and understanding a winter's seagrass foodweb network through effective trophic levels. *Ecological Modelling*, 117, 99–124.

Csardi, G. & Nepusz, T. (2006). The igraph software package for complex network research. *InterJournal*, Complex Systems, 1695.

Damuth, J. (1981). Population density and body size in mammals. *Nature*, 290, 699–700.

DeLong, J. P., Okie, J. G., Moses, M. E., Sibly, R. M. & Brown, J. H. (2010). Shifts in metabolic scaling, production, and efficiency across major evolutionary transitions of life. *Proceedings of the National Academy of Sciences*, 107, 12941–12945.

Dunne, J. A., Williams, R. J. & Martinez, N. D. (2002a). Food-web structure and network theory: The role of connectance and size. *Proceedings of the National Academy of Sciences*, 99, 12917–12922.

Dunne, J. A., Williams, R. J. & Martinez, N. D. (2002b). Network structure and biodiversity loss in food webs: Robustness increases with connectance. *Ecology Letters*, 5, 558–567.

Hechinger, R. F., Lafferty, K. D., McLaughlin, J. P., Fredensborg, B. L., Huspeni, T. C., Lorda, J., Sandhu, P. K., Shaw, J. C., Torchin, M. E., Whitney, K. L. & Kuris, A. M. (2011). Food webs

including parasites, biomass, body sizes, and life stages for three California/Baja California estuaries. *Ecology*, 92, 791–791.

Holling, C. S. (1959). Some Characteristics of Simple Types of Predation and Parasitism. URL http://www.journals.cambridge.org/abstract{_}S0008347X00072692.

Huxham, M., Beaney, S. & Raffaelli, D. (1996). Do Parasites Reduce the Chances of Triangulation in a Real Food Web? *Oikos*, 76, 284.

Johnson, S., Domínguez-García, V., Donetti, L. & Muñoz, M. a. (2014). Trophic coherence determines food-web stability. *Proceedings of the National Academy of Sciences*, 111, 17923–17928.

Jonhson, S., Domínguez-García, V. & Muñoz, M. A. (2013). Factors Determining Nestedness in Complex Networks. *PLoS ONE*, 8, e74025.

Jonsson, T., Cohen, J. & Carpenter, S. (2005). Food webs, body size, and species abundance in ecological community description. *Advances in Ecological Research*, 36, 1–84.

Kondoh, M. (2007). Anti-predator defence and the complexity-stability relationship of food webs. *Proceedings of the Royal Society B: Biological Sciences*, 274, 1617–1624.

Krause, A. E., Frank, K. A., Mason, D. M., Ulanowicz, R. E. & Taylor, W. W. (2003). Compartments revealed in food-web structure. *Nature*, 426, 282–285.

Lang, B., Ehnes, R. B., Brose, U. & Rall, B. C. (2017). Temperature and consumer type dependencies of energy flows in natural communities. *Oikos*, 126, 1717–1725.

Leaper, R. & Huxham, M. (2002). Size constraints in a real food web: Predator, parasite and prey body-size relationships. *Oikos*, 99, 443–456.

McLaughlin, Ó. B., Jonsson, T. & Emmerson, M. C. (2010). Temporal Variability in Predator–Prey Relationships of a Forest Floor Food Web. *Advances in Ecological Research*, 42, 171–264.

Oksanen, J., Blanchet, F. G., Friendly, M., Kindt, R., Legendre, P., McGlinn, D., Minchin, P. R., O'Hara, R. B., Simpson, G. L., Solymos, P., Stevens, M. H. H., Szoecs, E. & Wagner, H. (2018). *vegan: Community Ecology Package*. URL https://CRAN.R-project.org/package=vegan. R package version 2.5-2.

Opsahl, T. & Panzarasa, P. (2009). Clustering in weighted networks. *Social Networks*, 31, 155–163.

Pawar, S. (2015). The Role of Body Size Variation in Community Assembly. In: *Advances in Ecological Research*, vol. 52, 1st edn. Elsevier Ltd. ISBN 9780128024454, pp. 201–248. URL http://dx.doi.org/10.1016/bs.aecr.2015.02.003https://linkinghub.elsevier.com/retrieve/pii/S0065250415000094.

Pawar, S., Dell, A. I. & Van M. Savage (2012). Dimensionality of consumer search space drives trophic interaction strengths. *Nature*, 486, 485–489.

Petchey, O. L., Beckerman, A. P., Riede, J. O. & Warren, P. H. (2008). Size, foraging, and food web structure. *Proceedings of the National Academy of Sciences*, 105, 4191–4196.

Peters, R. H. (1986). *The ecological implications of body size*, vol. 2. Cambridge University Press.

Renaud, P. E., Tessmann, M., Evenset, A. & Christensen, G. N. (2011). Benthic food-web structure of an arctic fjord (kongsfjorden, svalbard). *Marine Biology Research*, 7, 13–26.

Ritchie, M. E. (2009). *Scale, heterogeneity, and the structure and diversity of ecological communities*, vol. 47. Princeton University Press.

Rizzuto, M., Carbone, C. & Pawar, S. (2018). Foraging constraints reverse the scaling of activity time in carnivores. *Nature Ecology & Evolution*, 2, 247–253.

Savage, V. M., Gilloly, J. F., Brown, J. H. & Charnov, E. L. (2004). Effects of body size and temperature on population growth. *The American Naturalist*, 163, 429–441.

Savage, V. M., Webb, C. T. & Norberg, J. (2007). A general multi-trait-based framework for studying the effects of biodiversity on ecosystem functioning. *Journal of Theoretical Biology*, 247, 213–229.

Tang, S., Pawar, S. & Allesina, S. (2014). Correlation between interaction strengths drives stability in large ecological networks. *Ecology Letters*, 17, 1094–1100.

Ulrich, W. & Gotelli, N. J. (2007). Null model analysis of species nestedness patterns. *Ecology*, 88, 1824–1831.

Vucic-Pestic, O., Rall, B. C., Kalinkat, G. & Brose, U. (2010). Allometric functional response model: body masses constrain interaction strengths. *Journal of Animal Ecology*, 79, 249–256.

Williams, R. J. & Martinez, N. D. (2000). Simple rules yield complex food webs. *Nature*, 404, 180–183.

Williams, R. J. & Martinez, N. D. (2004). Limits to Trophic Levels and Omnivory in Complex Food Webs: Theory and Data. *The American Naturalist*, 163, 458–468.

Wood, S. N. (2006). *Generalized additive models: an introduction with R*. Chapman and Hall/CRC.

Woodward, G., Ebenman, B., Emmerson, M., Montoya, J. M., Olesen, J. M., Valido, A. & Warren, P. H. (2005). Body size in ecological networks. *Trends in Ecology and Evolution*, 20, 402–409.

Zheng, J. X.-S., Pawar, S. & Goodman, D. F. M. (2018). Graph drawing by stochastic gradient descent. *IEEE transactions on visualization and computer graphics*.